Molecular Biology of the Cell
Vol. 18, 4446–4456, November 2007

ErbB4 Isoforms Selectively Regulate Growth Factor–induced Madin-Darby Canine Kidney Cell Tubulogenesis

Fenghua Zeng,* Ming-Zhi Zhang,* Amar B. Singh,* Roy Zent,*† and Raymond C. Harris*†

*Division of Nephrology and Hypertension, Department of Medicine, Vanderbilt University, Nashville, TN 37232; and †Nashville Veterans Affairs Hospital, Nashville, TN 37232

Submitted March 8, 2007; Revised July 31, 2007; Accepted August 15, 2007
Monitoring Editor: Keith Mostov

ErbB4, a member of the epidermal growth factor (EGF) receptor family that can be activated by heregulin β1 and heparin binding (HB)-EGF, is expressed as alternatively spliced isoforms characterized by variant extracellular juxtamembrane (JM) and intracellular cytoplasmic (CYT) domains. ErbB4 plays a critical role in cardiac and neural development. We demonstrated that ErbB4 is expressed in the ureteric buds and developing tubules of embryonic rat kidney and in collecting ducts in adult. The predominant isoforms expressed in kidney are JM-a and CYT-2. In ErbB4-transfected MDCK II cells, basal cell proliferation and hepatocyte growth factor (HGF)-induced tubule formation were decreased by all four isoforms. Only JM-a/CYT-2 cells formed tubules upon HB-EGF stimulation. ErbB4 was activated by both HRG-β1 and HB-EGF stimulation; however, compared with HRG-β1, HB-EGF induced phosphorylation of the 80-kDa cytoplasmic cleavage fragment of the JM-a/CYT-2 isoform. HB-EGF also induced early activation of ERK1/2 in JM-a/CYT-2 cells and promoted nuclear translocation of the JM-a/CYT-2 cytoplasmic tail. In summary, our data indicate that JM-a/CYT-2, the ErbB4 isoform that is proteinase cleavable but does not contain a PI3K-binding domain in its cytoplasmic tail, mediates important functions in renal epithelial cells in response to HB-EGF.

INTRODUCTION

ErbB4, a type I transmembrane receptor tyrosine kinase, belongs to the EGF receptor family, which consists of four receptors, ErbB1 (EGFR or HER1), ErbB2 (Neu, HER2), ErbB3 (HER3), and ErbB4 (HER4; Olayioye *et al.*, 2000). ErbB receptors are involved in the regulation of cellular proliferation, differentiation, survival, and migration in response to activation by their ligands (Yarden and Sliwkowski, 2001). The binding of receptor-specific ligands to the extracellular domains of the receptors results in the formation of homo- and hetero-dimeric receptor complexes and subsequent activation of intracellular signaling pathways (Olayioye *et al.*, 2000). More than a dozen ligands have been found to interact with the ErbB family receptors (Riese and Stern, 1998). Among these, ErbB4 ligands belong to two groups: the neuregulins (NRG1-4), also termed heregulins (HRG), and some members of the EGF family (betacellulin, epiregulin, and heparin-binding EGF-like [HB-EGF] growth factor) that were originally discovered as activators of ErbB1. NRG1 and NRG2 have a number of splice variants and also bind to ErbB3, whereas NRG3 and NRG4 interact with low affinity only with ErbB4 (Olayioye *et al.*, 2000). In most assays, NRG1, which contains a β-type (HRG-β1) EGF-like domain, has been found to be 10–100 times more potent than NRG2 with its α-type EGF-like domain (Beerli and Hynes, 1996; Riese *et al.*, 1996; Elenius *et al.*, 1997b; Falls, 2003). Based on these observations, HRG-β1 has been routinely utilized to stimulate ErbB4 activation.

ErbB4 is expressed as alternatively spliced isoforms that are characterized by variant extracellular juxtamembrane (JM) domains and intracellular cytoplasmic (CYT) domains. The JM domain of type a (JM-a) includes 23 amino acids that confer a proteinase cleavage site that is missing from the alternative 13 amino acids in the JM domain of type b (JM-b; Elenius *et al.*, 1997b; Gilmour *et al.*, 2001). Two additional JM splice variants (JM-c and JM-d) have recently been identified with isoforms lacking or including, respectively, both JM-a and JM-b sequences (Gilbertson *et al.*, 2001; Figure 1). Both JM-a and JM-d isoforms can be cleaved by ADAM 17, a member of the ADAM (a disintegrin and metalloprotease) family, also known as the tumor necrosis factor alpha-converting enzyme (TACE), in response to binding of ligands to ErbB4 (Zhou and Carpenter, 2000; Cheng *et al.*, 2003) or activation of protein kinase C (Vecchi *et al.*, 1996; Rio *et al.*, 2000). ErbB4 proteolytic cleavage releases a 120-kDa ectodomain fragment into the extracellular milieu and generates a membrane-associated 80-kDa fragment that can be degraded by proteasome activity after polyubiquitination (Vecchi and Carpenter, 1997) or can be further cleaved by γ-secretase, which releases the intracellular domain (ICD) from the membrane and allows nuclear translocation (Ni *et al.*, 2001; Lee *et al.*, 2002). Recent studies have shown that this ICD fragment can serve as a chaperone to facilitate the nuclear entry of the transcription factors STAT5a (56) and Yes-associated protein (YAP; Komuro *et al.*, 2003; Omerovic *et al.*, 2004).

The CYT isoforms differ by containing (CYT-1) or not containing (CYT-2) a sequence of 16 amino acids within their cytoplasmic tails (Elenius *et al.*, 1999). These 16 amino acids

This article was published online ahead of print in *MBC in Press* (http://www.molbiolcell.org/cgi/doi/10.1091/mbc.E07–03–0223) on August 29, 2007.

Address correspondence to: Raymond C. Harris (ray.harris@vanderbilt.edu).

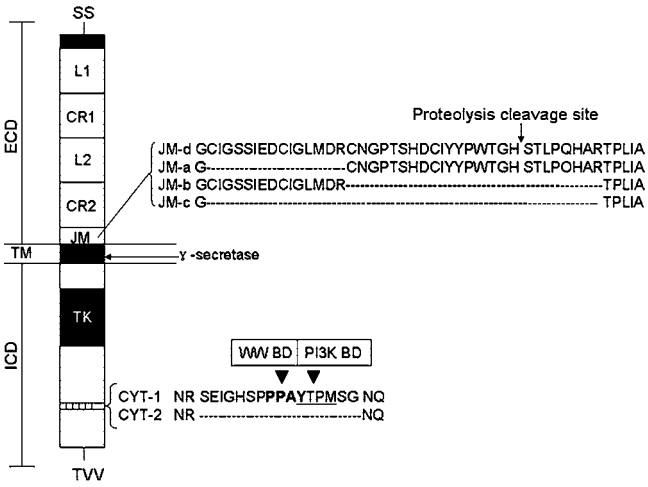

Figure 1. Schematic illustration of ErbB4 structure and isoforms. All the isoforms contain extracellular ligand binding domain (ECD), juxtamembrane (JM), transmembrane (TM) and a intracellular domain (ICD). ECD contains a signal sequence (SS), two ligand-interacting domains (L1, L2) and two cysteine-rich (CR) domains. JM contains alternative JM isoforms, with (JM-d, JM-a) or without (JM-b, JM-c) a proteolytic cleavage site between His651 and Ser652. ICD contains a tyrosine kinase domain (TK), a regulatory domain with autophosphorylation sites plus sequence changes attributable to the CYT-1 and CYT-2 isoforms (hatched box). CYT-2 isoform has a 16-amino acid deletion that contains a PI3K-binding (PI3K BD, underlined) and a WW domain binding (WW BD, bold) motif. Dashes represent deletions.

(SEIGHSPPPAYTPMSG) can serve as a binding site for the phosphatidylinositol 3-OH kinase (PI3K) SH2-domain (YTPM) and putatively for WW-domain containing signaling molecules (PY motif, PPXY, where X stands for any amino acid; Carpenter, 2003; Komuro *et al.*, 2003; Figure 1). Previous studies have reported differential coupling and activation of PI3K signaling between these two cytoplasmic variants (Kainulainen *et al.*, 2000).

In vivo, ErbB4 isoforms are expressed in a tissue-specific distribution. For example, ErbB4 JM-b is expressed mainly in the heart and ErbB4 JM-a mainly in kidney, whereas both juxtamembrane isoforms are expressed in various neural tissues (Elenius *et al.*, 1997a). On the other hand, heart expresses predominantly ErbB4 CYT-1; neural tissues and kidney predominantly ErbB4 CYT-2 (Elenius *et al.*, 1999). The tissue-specific expression of ErbB4 isoforms suggests that a level of specificity in isoform-specific function might exist.

The function of ErbB4 appears to vary depending on its context. ErbB4 has been shown to have an important role in cardiac and neural development. ErbB4 knockout mice died at midembryogenesis (embryonic day [E] 10.5) before the inception of nephrogenesis, due to impaired cardiac muscle differentiation and defects in pathfinding by cranial neural crest cells and in the migration of cerebellar granule cells along radial glial fibers (Gassmann *et al.*, 1995). Therefore, its role in renal development could not be assessed. We previously found that the ErbB4 ligands, HRG-β1 (Harris, unpublished data) and HB-EGF, were expressed in the ureteric bud as early as E14.5, and there was persistent expression in structures arising from the ureteric bud throughout embryogenesis (Sakai *et al.*, 1997), which raised questions concerning the pattern of ErbB4 expression and possible functions in renal development and epithelial function. Furthermore, because PI3K signaling has been shown to have important roles in mediating cell survival and proliferation and ureteric bud growth in vitro (Grant *et al.*, 2002; Brader and Eccles, 2004; Pozzi *et al.*, 2006), we initially hypothesized that the ErbB4 variant containing the PI3K binding site (CYT-1) might serve as a mediator of epithelial tubulogenesis. However, in the present study, we demonstrate that in both developing and adult kidney, the predominant ErbB4 isoforms expressed was CYT-2, which does not contain the PI3K-binding site. We found that in Madin-Darby canine kidney (MDCK) II cells, transfection of all ErbB4 isoforms inhibited basal proliferation, whereas cell adhesion and migration were differentially regulated. HGF-induced tubulogenesis was also inhibited by the expression of ErbB4 isoforms, but unexpectedly, CYT-2, the ErbB4 isoform without PI3K-binding site, induced tubulogenesis upon HB-EGF treatment, which correlated with selective HB-EGF–mediated receptor phosphorylation and nuclear translocation of this isoform.

MATERIALS AND METHODS

Cell Culture and Transfection

MDCK II cells were cultured at 37°C in a humidified air atmosphere with 5% CO_2. DMEM/F12 (Invitrogen, Carlsbad, CA), supplemented with 10% fetal bovine serum, streptomycin (100 μg/ml), and penicillin (100 U/ml), was used as growth medium. The medium used for passage of the transfected cell lines was supplemented with 1 mg/ml G418 (Research Products International, Mount Prospect, IL).

The expression constructs encoding full-length human ErbB4 cloned in the pcDNA3.1 were kindly provided by Dr. Klaus Elenius (Department of Oncology, Turku University, Turku, Finland) and were sequenced after reamplification. To develop cells stably expressing human ErbB4 isoforms, MDCK II cells were transfected with pcDNA3.1 containing human ErbB4 isoform cDNAs, using Effectene Transfection Reagent (QIAGEN, Chatsworth, CA) according to the manufacturer's instruction. Stable transfectants were generated after selection with 1 mg/ml G418 for 3 to 4 wk. Positive clones were confirmed by immunoblotting with anti-ErbB4 antibody as described below, and two independent clones were studied for each construct.

Antibodies and Reagents

Recombinant human NRG-1-β1/HRG-β1 EGF domain was purchased from R&D Systems (Minneapolis, MN). Recombinant human HGF was from Chemicon International (Temecula, CA). HB-EGF, leptomycin B (LMB), and phorbol 13-myristate 12-acetate (PMA) were from Sigma-Aldrich (St. Louis, MO). Anti-ErbB4 (c-18), anti-phospho-ERK1/2 (42/44), and anti-phosphotyrosine (PY99) were purchased from Santa Cruz Biotechnology (Santa Cruz, CA). Anti-ErbB4 antibodies (Ab-2) were from Neomarkers (Fremont, CA). Both ErbB4 antibodies (c-18 and Ab2) were raised against ErbB4 c-terminus and can recognize all splice variants of ErbB4. Anti-phospho-ErbB4^{tyr1284}, anti-phospho-Akt^{Ser473}, and anti-phospho-STAT3^{Tyr705} were from Cell Signaling Technology (Beverly, MA). Rat tail collagen, type 1, was from BD Biosciences (San Jose, CA) and TO-PRO-3 iodide from Molecular Probes (Invitrogen).

Unless otherwise noted, antibodies were used at 1:200 for immunostaining and 1:1000 for immunoprecipitation and Western blot.

Immunohistochemistry

Immunohistochemistry was performed as previously described (Zhang *et al.*, 2004).

Real-Time PCR

Total RNA was isolated from embryonic or adult Sprague Dawley (SD) rat kidneys by the TRIzol reagent (Invitrogen) and was subsequently reverse-transcribed to cDNA with Superscript II enzyme according to the manufacturer's instructions using random oligonucleotide primers (GIBCO-BRL, Rockville, MD).

Real-time PCR analysis of cDNA samples was performed with specific primers and fluorescent probes designed using the Beacon Designer 2 and synthesized by Sigma-Genosys (Table 1). Each probe was double-labeled with the fluorescent reporter dye (6FAM) linked to the 5′-end of the probe and the black hole quencher dye (BHQ1) attached to the 3′-end. Quantitative PCR was performed in 96-well reaction plates using iCycler iQ Real Time PCR System (Bio-Rad, Richmond, CA). The reaction mixture contained an amount of cDNA corresponding to 200 ng of reverse-transcribed total RNA (20 ng for ubiquitin), 400-nm sense and antisense primers, and 200-nm probe in a final volume of 25 μl using the TaqMan PCR mix (Applied Biosystems, Foster City, CA). Cycle parameters were 95°C × 15 min and then 40 cycles of 94°C for 15 s

Table 1. Sequences of primers and probes for RT-PCR

Target mRNA	GenBank number	Primer/probe	Sequence
ErbB4 JM-a	AY375306	Forward	5′-AGTGCCACCCTTGCCATC-3′
		Reverse	5′-AGAGCCATGATGACCAGGATG-3′
		Probe	5′-ATGGACGGGCCATTCCACTTTACCA-3′
ErbB4 JM-c	AY375306	Forward	5′-AGTGCCACCCTTGCCATC-3′
		Reverse	5′-AGAGCCATGATGACCAGGATG-3′
		Probe[a]	5′-CTGCACCCAGGGAACTCCACTGAT-3′
ErbB4 CYT-1	AY375306	Forward	5′-ACCTCCTATCTACACATCCAGAAC-3′
		Reverse	5′-GGCATGGGCATTCCTTGTTG-3′
		Probe	5′-TGAAATTGGACACAGCCCTCCTCCTG-3′
ErbB4 CYT-2	AY375306	Forward	5′-ACCTCCTATCTACACATCCAGAAC-3′
		Reverse	5′-GGCATGGGCATTCCTTGTTG-3′
		Probe[b]	5′-AATTGACTCCAATAGGAATCAGTTTGTGTACCAGGAT-3′
Ubiquitin	BC060312	Forward	5′-CCGGCGGGCACTGAT-3′
		Reverse	5′-CATTTTTAACAGAGGTTCAGCTATTACTG-3′
		Probe	5′-CATTACTCTGCACTCTAGCCATTTGCCCC-3′

[a] The sequence for the ErbB JM-c probe was designed according to our sequence results.
[b] The GenBank number for the ErbB4 CYT-2 probe sequence is AY375307.

and 60°C for 60 s. Each sample was run in triplicate. Relative quantitation of a given gene was calculated after normalization to the ubiquitin amount. Individual Ct values are means of triplicate measurements. Delta Ct (dCt) was calculated by subtraction of the ubiquitin Ct value from the individual Ct value, and then converted to arbitrary values with the formula: arbitrary units = $2^{-dCt} \times 10^3$, assuming an efficiency of amplification of 100%. Results are expressed as mean ± SE of three experiments.

Immunoblot Analysis

For cell culture, cells were prepared as follows: 1) for detection of the ErbB4 receptor expression levels, cells in exponential growth phase were trypsinized and 1×10^6 cells were plated on 10-cm tissue culture dishes for 18 h before harvesting; 2) For detection of the level of tyrosine phosphorylated ErbB4 receptors, cells were grown to 80% confluence and starved overnight in serum-free DMEM/F12 containing 0.1% bovine serum albumin (BSA). After stimulation with 50 ng/ml HRG-β1 or HB-EGF for 10 min at 37°C, cells were washed three times with ice-cold Ca^{2+}- and Mg^{2+}-free phosphate-buffered saline (PBS) and lysed with ice-cold TGH buffer (1% Triton X-100, 10% glycerol, 20 mM HEPES, pH 7.2, 100 mM NaCl, 1 mM phenylmethylsulfonyl fluoride, 10 μg/ml leupeptin, 10 μg/ml aprotinin, and 1 mM Na_3VO_4). The lysates were incubated for 20 min on ice with intermittent vortexing. Insoluble material was removed by centrifugation (14,000 × *g*, 15 min) at 4°C, and the supernatant was collected. Protein concentrations were assayed by the method of Bradford using BSA as the standard. For immunoprecipitation, ~1 μg of ErbB4 antibody (c-18) or PY99 antibody was incubated (2 h at 4°C) with 500 μg of cellular protein followed by overnight incubation with protein G-agarose (Invitrogen). Immune complexes were washed three times with TGH lysis buffer, resuspended in 2× Laemmli buffer, and boiled for 5 min. 3) For testing the phosphorylation level of Akt, ERK1/2, and STAT3, cells were serum-starved for 24 h before seeding into collagen I solution (see below) at a concentration of 60,000 cells/100 μl collagen I solution that contained 50 ng/ml HRG-β1 or HB-EGF. Cells in collagen gel solution without growth factors were used as control. At different time points, 20 μl of 6× SDS sample buffer was added, and the cell-gel mixture was sonicated and boiled for 5 min. Equal volumes of each sample were loaded.

After SDS-PAGE, the proteins were transferred to polyvinylidene fluoride (PVDF) membranes for Western blotting. Immunoblots were blocked with TBST buffer (0.05% Tween 20, 150 mM NaCl, 50 mM Tris, pH 7.4) containing 5% nonfat milk powder (blocking buffer) at room temperature for 1 h. The membranes were probed overnight at 4°C with phospho-antibodies in TBST containing 3% BSA or total antibodies in blocking buffer, washed three times with TBST buffer, and incubated with peroxidase-conjugated secondary antibody. After thorough washing, the chemiluminescence reaction was performed, and the membranes were exposed to electrochemiluminescence (ECL) hyperfilm according to the manufacturer's instructions (Amersham Pharmacia Biotech, Piscataway, NJ). Levels of protein phosphorylation of the ErbB4 80-kDa cleavage fragment were quantitated with an IS-1000 digital imaging system (Alpha Innotech, San Leandro, CA).

For detection of ErbB4 expression levels in developing rat kidney, tissues were homogenized in ice-cold TGH buffer. Equal amounts of protein (100 μg) were loaded and blotted with ErbB4 Ab-2 antibody. For immunoprecipitation, 2 mg protein was immunoprecipitated with ErbB4 c-18 antibody and blotted with ErbB4 Ab-2 antibody.

Collagen Gel Culture

MDCK tubulogenesis assays were performed in three-dimensional (3D) extracellular matrix gels as previously described (Cantley *et al.*, 1994; Chen *et al.*, 2004). In brief, cells were suspended at 2×10^3 cells/100 μl in a neutralized collagen I solution that was composed of 1.5 mg/ml collagen I in DMEM/F12 containing 20 mM HEPES (pH 7.2) and were dispensed into 96-well plates and incubated at 37°C. After the collagen I solution had solidified, the complete culture medium with HGF, 20 ng/ml; HRG-β1, 50 ng/ml; or HB-EGF, 50 ng/ml was added and renewed every day. One group of cells without growth factors served as control. Cysts and tubules were photographed after 9–10 d of culture under phase contrast using a Nikon Diaphot TMD inverted microscope (Melville, NY).

Cell Proliferation

Cell proliferation was performed in 3D collagen I solution as previously described (Mai *et al.*, 2005). Briefly, 6×10^4 cells embedded in 100 μl collagen I solution were plated in 96-well plates as described in tubulogenesis and incubated in DMEM/F12 containing 5% fetal bovine serum (FBS) with or without (control) HRG-β1, 50 ng/ml, or HB-EGF, 50 ng/ml, after pretreatment with the PI3K inhibitor LY294002 5 μM or mitogen-activated protein kinase (MAPK) inhibitor U0126 5 μM for 2 h. Medium was changed everyday with corresponding growth factors and inhibitors. After 72 h, cells were pulsed with [^{3}H]thymidine (1 μCi/well) for 24 h before collection. The gels were then removed from the plates and dialyzed against PBS for 24 h to remove free [^{3}H]thymidine. The cells in the gels were then lysed in 10% SDS, and ^{3}H radioactivity was measured in a scintillation counter.

Cell Adhesion

Microtiter plates (U-bottomed, 96-well) were coated with collagen I at the indicated concentrations in PBS for 1 h at 37°C. Plates were then washed with PBS and incubated with PBS containing 0.1% BSA for 60 min to block nonspecific adhesion. Cells (n = 100,000) in 100 μl serum-free DMEM were added in triplicate to 96-well plates and incubated for 1 h at 37°C, the time necessary for MDCK to adhere maximally to collagen I (data not shown). Nonadherent cells were removed by washing the wells with PBS. Cells were then fixed with 3.7% formaldehyde, stained with 1% crystal violet, and solubilized in 20% acetic acid, and the optical density (OD) of cell lysates was read at 570 nm. Cells bound to fetal calf serum were used as a positive control to indicate maximal cell adhesion, whereas cells bound to 1% BSA-coated wells were used as background. The percentage of cell adhesion was calculated as (OD of test − OD of the background)/(OD of the positive control − OD of the background).

Cell Motility Assay

Cell motility was measured by a transwell migration assay carried out in transwells consisting of PVDF-free polycarbonate filters with 8-μm pores (Corning Costar, Acton, MA). The underside of each transwell was precoated with 10 μg/ml collagen I overnight at 4°C, and the filter was subsequently blocked with 1% BSA for 1 h at 37°C to inhibit nonspecific migration. Cells, 5×10^4, in 100 μl serum-free medium were added to the upper wells and were then allowed to migrate into the matrix coated on the underside of the

transwell for 4 h. Cells on the top of the filter were removed by wiping with a cotton swab, and the filter was then fixed in 3.7% formaldehyde in PBS. Migrating cells were stained with 1% crystal violet, and five random fields of view at 400× magnification were counted and expressed as the average number of cells per field of view. Three independent experiments were performed and the data were represented as mean ± SE.

Immunofluorescence Staining

Cells plated on glass coverslips were rinsed in PBS++ (PBS plus 0.5 mM $MgCl_2$ and 0.9 mM $CaCl_2$) and fixed with 4% paraformaldehyde in PBS++ for 30 min on ice. The fixed cells were permeabilized with 0.2% Triton X-100 in PBS++ for 2 min at room temperature and washed three times with PBS++. After blocking with 5% normal goat serum and 1% BSA in PBS++, samples were incubated with primary antibodies overnight at 4°C in a moist chamber. Samples were then washed three times with PBS++, followed by incubation for 30 min with the respective conjugated second antibody (Jackson ImmunoResearch Laboratories, West Grove, PA). After three washes, cells were counterstained with TO-PRO-3 in PBS for 10 min and mounted with VectaShield mounting media (Vector Laboratories, Burlingame, CA). The images were examined using a Zeiss-410 confocal microscope (Thornwood, NY) at the Vanderbilt Imaging Core facility.

Statistics

Graphic data are presented as mean ± SE. Student's *t* test was used for comparing different treatments and cell lines. Differences with $p < 0.05$ were considered statistically significant.

RESULTS

Expression and Localization of ErbB4 Isoforms in Rat Embryonic and Adult Kidney

The expression and localization of ErbB4 were examined in rat embryonic and adult kidneys. As shown in Figure 2A, ErbB4 expression was weakly detected by immunoblotting in rat metanephric kidney at E15 and was strongly expressed at E19. After birth, ErbB4 expression levels decreased. At postnatal day (P) 6 and in adult rats, ErbB4 protein expression was detected mainly in renal medulla.

ErbB4 was immunolocalized to ureteric bud derivatives in E17.5 embryos (Figure 2B), similar to the localization previously reported for its ligands, HB-EGF and heregulin (Sakai *et al.*, 1997; Takemura *et al.*, 2002). In adult kidney, ErbB4 was mainly expressed in the distal nephron and in epithelial cells of the cortical and medullary collecting duct (Figure 2, C and D).

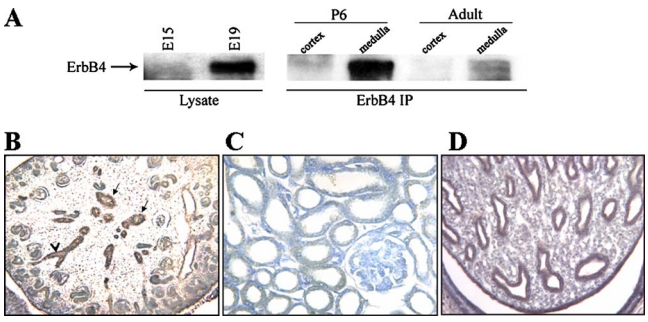

Figure 2. Expression of ErbB4 in rat embryonic and adult kidney. (A) Western blot analysis of ErbB4 expression level. Homogenates from kidney tissue at different stages of development or adult kidney cortex or medulla were separated by 7.5% SDS-PAGE and immunoblotted with ErbB4 antibody. ErbB4 had the highest expression level in the metanephric embryonic kidney (E19). In adult kidney ErbB4 was mainly expressed in medulla. IP, immunoprecipitation. (B–D) Immunohistological staining showed that ErbB4 protein was localized predominantly in the derivatives of the ureteric buds, including developing medullary collecting ducts (arrows) and branching ducts in the cortex (arrowhead) in metanephros of embryonic kidney day 17.5 (B), some distal ducts (C), and the collecting ducts in adult kidney (D). Brown (DAB stain) indicates ErbB4 immunoreactivity; Blue (toluidine blue), nuclei.

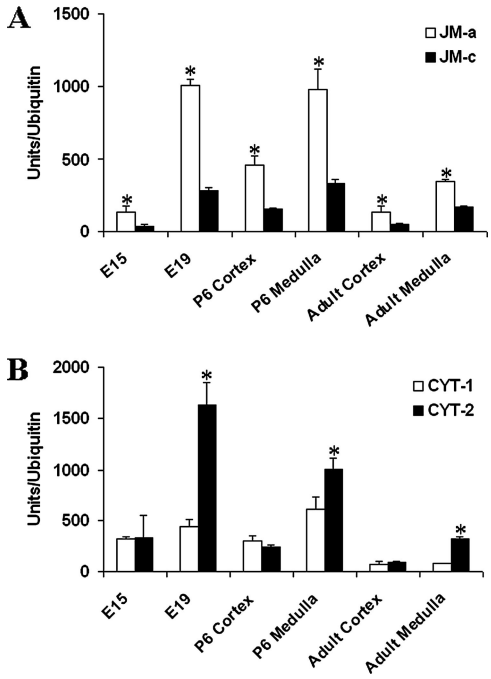

Figure 3. Quantitation of ErbB4 isoform mRNA level in rat development kidney by real-time PCR. ErbB4 JM isoforms (A) and CYT isoforms (B) were detected using specific primers and probes. Data were normalized to ubiquitin mRNA, which was used as internal control. Delta Ct was converted to arbitrary values by the formula $2^{-dCt} \times 10^3$. Results were expressed as mean ± SE of three experiments.

To investigate which ErbB4 isoforms were expressed during renal development, real-time PCR was performed using primers flanking the rat ErbB4 juxtamembrane domain or CYT-1 site and specific probes for each isoform. From E15 to adult, four ErbB4 isoforms were detected: JM-a, JM-c, CYT-1, and CYT-2, with JM-a being the main juxtamembrane isoform and CYT-2 the predominant cytoplasmic isoform (Figure 3, A and B). At E19 the postnatal medulla exhibited the highest levels of expression of mRNA for JM-a and CYT-2, which corresponded to the ErbB4 protein expression level detected by immunoblotting. The identities of the amplified RT-PCR products were also confirmed by cloning the single ErbB4 JM or CYT RT-PCR products and sequencing the inserts.

ErbB4 Clone Selection and Phosphorylation Induced by HRG-β1 and HB-EGF

In preliminary studies, we determined that commonly utilized cell lines derived from either adult collecting duct (IMCD cells) or ureteric bud (UB cells) failed to express detectable levels of endogenous ErbB4. Like IMCD and UB cells, MDCK II cells, another well-characterized polarized renal epithelial cell line, also does not express endogenous ErbB4. Furthermore, they do not spontaneously form tubules when grown in collagen gels in the presence of fetal calf serum, which allows us to determine the effects of specific growth factors on tubulogenesis. Therefore, we transfected full-length human ErbB4 cDNA isoforms into MDCK II cells, selected stably transfected cell lines, and

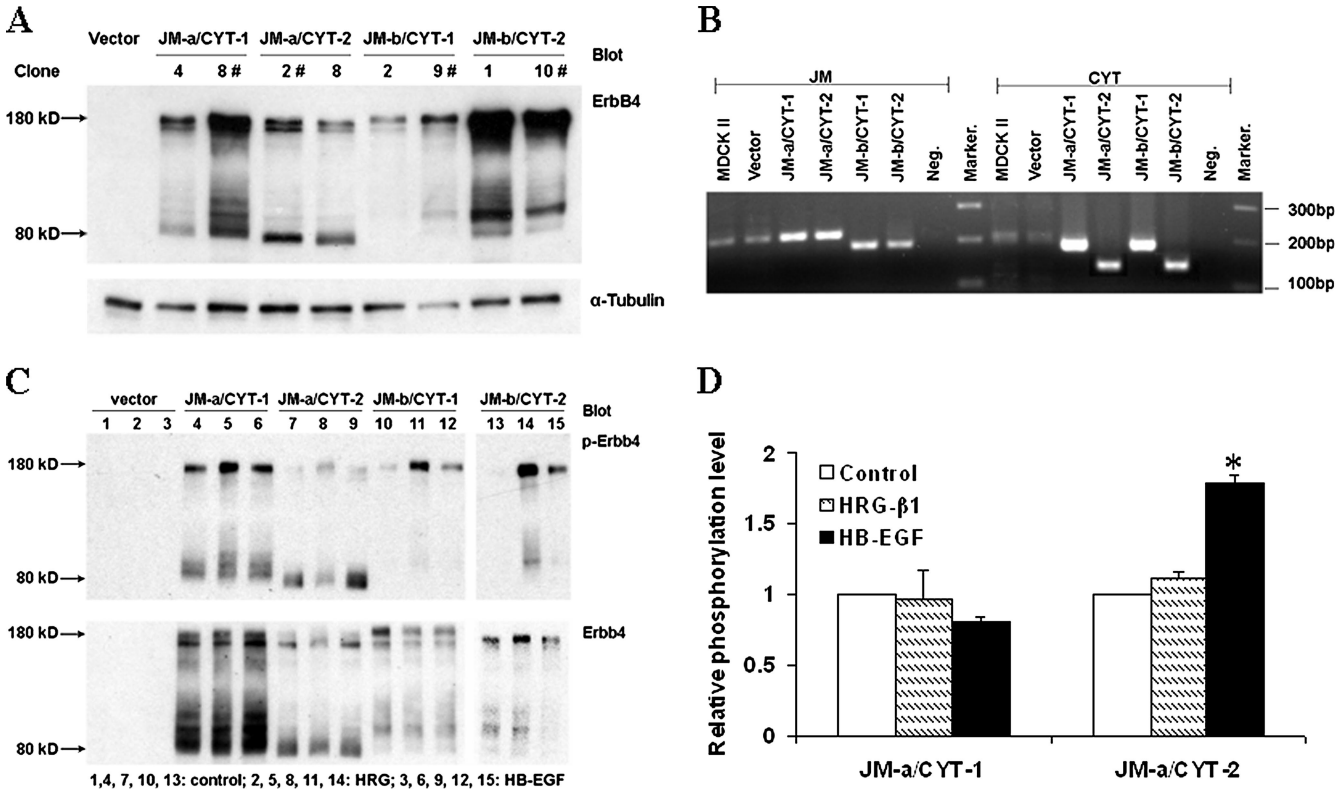

Figure 4. ErbB4 clone selection and phosphorylation induced by HRG-β1 and HB-EGF. (A) Representative clones with vector or ErbB4 JM-a/CYT-1, JM-a/CYT-2 or JM-b/CYT-1, or JM-b/CYT-2 expression levels by blot with ErbB4 c-18 antibody. Clones (marked by #) with relatively similar ErbB4 expression level were used for further studies. (B) ErbB4 isoform transfection was confirmed by RT-PCR using primers flanking human ErbB4 JM or CYT fragments. The expected size for the amplified ErbB4 JM-a isoform is 220 bp and JM-b is 190 bp. CYT-1 is 182 bp and CYT-2 is 134 bp. Neg, negative control. (C) Stimulation of ErbB4 phosphorylation by HRG-β1 or HB-EGF in MDCK II cells overexpressing ErbB4 isoforms. Cells were serum starved 24 h before treatment with HRG-β1 or HB-EGF for 10 min in 37°C. Immunoblotting was performed with anti-phospho-ErbB4 (p-ErbB4, top panel) and reblotted with ErbB4 antibody (bottom panel). (D) Relative protein phosphorylation level of the ErbB4 80-kDa cleavage fragment was calculated by correction for the total amount of the cleavage fragment and then compared with the control group. *$p < 0.05$ compared with control.

confirmed ErbB4 expression levels by immunoblotting (Figure 4A). In the ErbB4 JM-a isoform transfectants, a 180-kDa full-length ErbB4 band and a cleaved 80-kDa band were observed, indicating that both the JM-a/CYT-1 and JM-a/CYT-2 isoforms could be cleaved in the normal growth medium. ErbB4 CYT-2 transfectants had bands of a smaller molecular weight than CYT-1 due to the 16-amino acid deletion (in both full-length and 80-kDa bands). The noncleavable ErbB4 JM-b isoform transfectants only expressed the full-length 180-kDa band (Figure 4A). In all the isoforms, especially in the JM-b/CYT-2 isoform, a band around 100 kDa was also detected. Whether this band represents ErbB4 degradation or belongs to the truncated form of ErbB4 has not yet been determined. The specificity of each transfected isoform was confirmed by RT-PCR (Figure 4B).

To demonstrate that the ErbB4 proteins expressed by the transfectants were functional, cells were stimulated with 50 ng/ml HRG-β1 or 50 ng/ml HB-EGF for 10 min, and the phosphorylation level of ErbB4 was examined. As shown in Figure 4C, tyrosine phosphorylation of all ErbB4 isoforms increased in response to HRG-β1 and HB-EGF stimulation, although the response to HB-EGF was less pronounced. Of interest, the JM-a/CYT-2 isoform uniquely demonstrated increased phosphorylation of the 80-kDa cytoplasmic cleavage fragment upon HB-EGF treatment (Figure 4, C and D).

Expression of ErbB4 Isoforms Affects Tubulogenesis

When cultured in 3D collagen gels in the presence of fetal calf serum, MDCK II cells form cysts. Addition of HGF will induce tubule formation from single MDCK II cells or genetically homogenous epithelial cell clusters in collagen gels (Montesano *et al.*, 1991; Santos and Nigam, 1993; Stuart *et al.*, 1995; Balkovetz, 1998). Unlike other cell lines derived from renal epithelium, wild-type MDCK II cells do not form tubules in response to ligand-mediated ErbB1 activation (Barros *et al.*, 1995). In the presence of serum but the absence of HGF, all ErbB4 isoform-transfected cells exhibited a dramatic decrease in the size of cysts compared with vector-transfected cells (Figure 5). In the presence of HGF, vector-transfected MDCK II cells (control) exhibited the expected branching tubulogenesis (Figure 5). All ErbB4 isoforms had decreased tubulogenesis in response to HGF administration compared with control cells. However, there were distinctly different patterns among the four isoforms. JM-a/CYT-1 cells developed into elongated tubules with minimal branching; JM-a/CYT-2 cells separated from each other and formed extensive, long cell protrusions, but no tubule formation was ever noted; JM-b/CYT-1 cells formed oblong tubule-like cysts; and JM-b/CYT-2 cells developed minimally branching tubules similar to JM-a/CYT-1 cells.

HRG-β1 administration was unable to induce tubulogenesis in MDCK II cells. Instead, it induced cyst growth both in

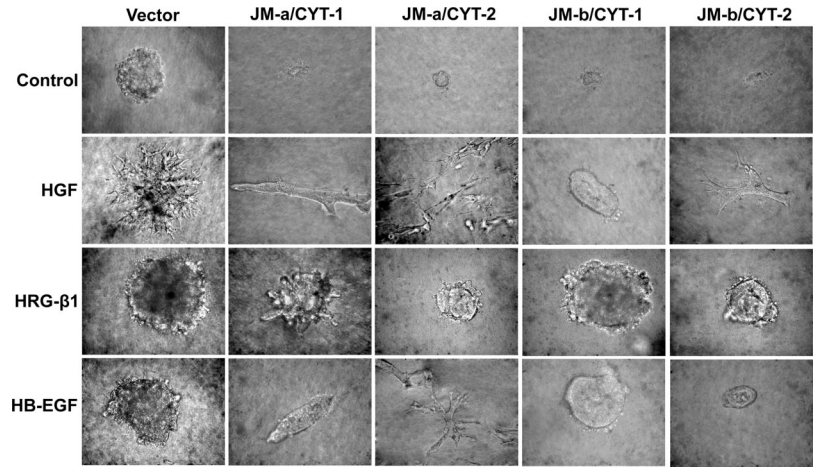

Figure 5. Cyst formation and tubulogenesis in ErbB4-transfected MDCK cells grown in collagen. Experiments were performed as described in *Materials and Methods.* After 9–10 d of culture, cells were fixed with 3.7% formaldehyde and photographed. From top to bottom: no treatment and growth in the presence of HGF (20 ng/ml), HRG-β1 (50 ng/ml), or HB-EGF (50 ng/ml). These findings were representative of at least four independent experiments.

the vector-transfected cells and in all four isoforms of ErbB4-transfected cells. Although vector-transfected cells did not express ErbB4, MDCK II cells do express abundant ErbB3, as well as ErbB2 (not shown). Because HRG-β1 does not activate EGFR (ErbB1), it is likely that the HRG-β1–induced cyst growth was mediated through ErbB3-mediated pathways. Of note, the HRG-β1–mediated cysts from JM-a/CYT-1 cells demonstrated many small-spike or needle-shaped outgrowths, although no typical tubular formations were ever detected. EGF administration also failed to induce tubulogenesis in MDCK II cells expressing any of the four ErbB4 isoforms (data not shown). In contrast, in response to HB-EGF treatment, JM-a/CYT-2 cells formed tubules, whereas all the other transfected cells, including vector control cells, only formed cysts.

ErbB4 Expression Inhibits Cell Proliferation

Decreased cyst formation in 3D collagen gel culture (Figure 5) suggested that ErbB4 overexpression might inhibit MDCK II cell proliferation. Cell proliferation was determined by measuring [^{3}H]thymidine incorporation in the 3D collagen gel culture in DMEM/F-12 containing 5% FBS. After 4-d culture in 3D collagen gels, all four ErbB4 isoforms tested had significantly inhibited thymidine incorporation compared with vector-transfected cells (Figure 6A). JM-a/CYT-1 and JM-a/CYT-2 cells were further examined for their responses to HRG-β1 or HB-EGF treatment. Because of the significant differences in the basal proliferation levels between vector and ErbB4 expressing cells (Figure 6A), the effects of growth factors or inhibitors were examined using relative proliferation ratios corresponding to each cell type's basal growth rate. As shown in Figure 6B, compared with cells without growth factor addition, both HRG-β1 and HB-EGF stimulated JM-a/CYT-1 and JM-a/CYT-2 cell proliferation ($p < 0.05$). Interestingly, the JM-a/CYT-2 cells had significantly increased thymidine incorporation in response to HB-EGF compared with HRG-β1 ($p < 0.05$), whereas the opposite pattern was noted in JM-a/CYT-1 cells ($p < 0.05$). Both HRG-β1– and HB-EGF–mediated cell proliferation were reduced by either a PI3K inhibitor (PY294002) or a MAPK inhibitor (U0126).

Expression of ErbB4 JM-a/CYT-2 Promotes MDCK Cells Attachment to Collagen I and Increases Cell Motility

We also investigated the effects of expression of ErbB4 isoforms on MDCK II cell adhesion to collagen I. As shown in Figure 7A, compared with vector alone or JM-a/CYT-1– and JM-b/CYT-1–transfected cells, both JM-a/CYT-2 and JM-b/CYT-2 were much more adherent at concentrations of collagen I from 0.625 to 5 μg/ml.

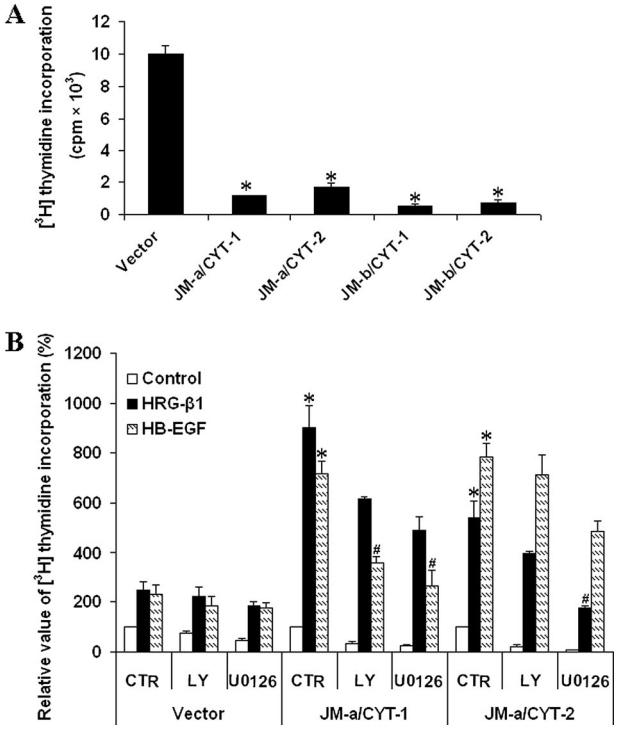

Figure 6. ErbB4 expression inhibited MDCK II cell proliferation. Cell mitogenesis was determined by [^{3}H]thymidine incorporation assays performed in a 3D collagen gel mixture as described in *Material and Methods.* (A) All four ErbB4 isoforms significantly inhibited MDCK II cell proliferation. Values are means ± SE of three independent experiments in triplicate wells. (B) Both HRG-β1– and HB-EGF–stimulated JM-a/CYT-1 and JM-a/CYT-2 cell proliferation. Interestingly, the JM-a/CYT-2 cells had significantly increased [^{3}H]thymidine incorporation in response to HB-EGF compared with HRG-β1, whereas the opposite effect was noted in JM-a/CYT-1 cells. Growth factor–mediated cell proliferation was reduced by both the PI3K inhibitor (LY294002) and the MAPK inhibitor (U0126). Values represent ratios compared with controls (no treatment, 100%). CTR, control; LY, LY294002. *$p < 0.05$ versus corresponding control group; #$p < 0.05$ versus corresponding growth factor treatment group without inhibitors.

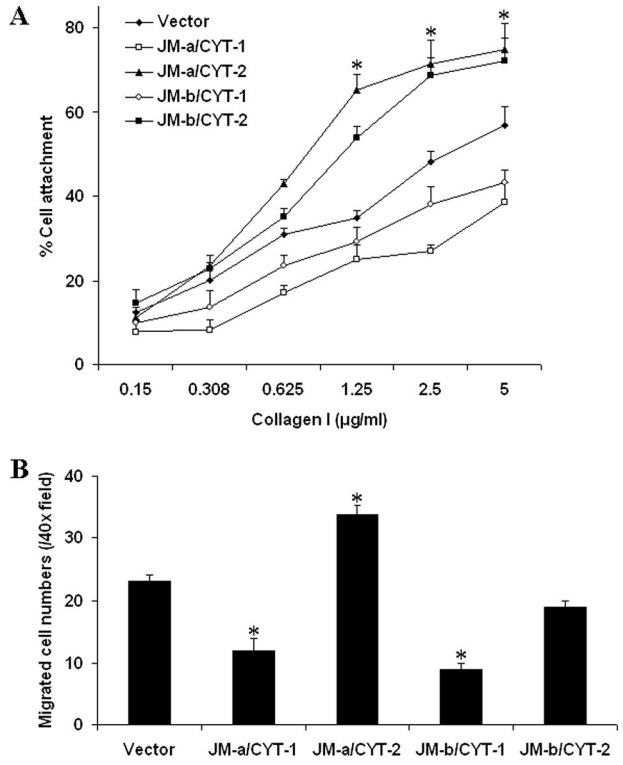

Figure 7. Cell attachment and migration of ErbB4-transfected MDCK cells. (A) Effect of ErbB4 expression on attachment of MDCK II cells. Adhesion assays were performed on collagen I–coated plates as described in *Materials and Methods.* The results were the average of four independent experiments ± SE, each with three replications. JM-a/CYT-2 and JM-b/CYT-2 cells showed significantly increased cell–matrix adhesion compared with vector alone or JM-a/CYT-1 and JM-b/CYT-1 cells. (B) Expression of ErbB4 altered the migration of MDCK II cells in a modified Boyden chamber migration assay. MDCK II cells were placed in transwell filter chambers coated on the underside with collagen I. Cells were then allowed to migrate for 4 h and were quantitated as described in *Materials and Methods.* *$p < 0.05$ compared to vector alone cells.

Increased cell–matrix interactions may also affect cell chemotaxis and motility (Hotchkiss et al., 2005). To investigate whether ErbB4 expression affected MDCK II cell motility, we used a transwell migration assay. MDCK II vector or ErbB4-expressing cells were placed in the upper chamber of transwell filters that had been coated on the underside with 5 μg/ml collagen I solution and were allowed to migrate for 4 h. Compared with vector-transfected cells, ErbB4 JM-a/CYT-2 expression significantly increased and JM-a/CYT-1 and JM-b/CYT-1 expression decreased cell motility (Figure 7B). The expression of the ErbB4 JM-b/CYT-2 isoform yielded results that were indistinguishable from controls.

HB-EGF Treatment Strongly Activated ERK1/2 Phosphorylation at Early Phases of Tubulogenesis in JM-a/CYT-2 Cells

Formation of branched tubular structures in epithelial cells induced by HGF requires distinct temporal responses (Medico *et al.*, 1996; Sachs *et al.*, 1996). The first phase of the response (scattering), which results from cytoskeletal reorganization, loss of intercellular junctions, and cell migration, is dependent on PI3K and Rac activation (Ridley *et al.*, 1995; Royal and Park, 1995). The second phase (growth) requires stimulation of the Ras-MAPK cascade (Ponzetto *et al.*, 1996; O'Brien *et al.*, 2004). The third phase (tubulogenesis) is dependent on the STAT (signal transducers and activators of transcription) pathway (Boccaccio *et al.*, 1998). HGF stimulates recruitment of STAT3 to the HGF receptor, tyrosine phosphorylation, nuclear translocation, and binding to the specific promoter element, Sis-inducible element (SIE). Therefore, we determined whether these pathways were altered in ErbB4-overexpressing MDCK II cells grown in collagen gels. We found that phospho-Akt levels were increased in both CYT-1 and -2, as well as vector alone transfected cells upon HRG-β1 treatment, but not in response to HB-EGF treatment. Given that MDCK II cells also express ErbB3 receptors, which stimulates PI3K upon activation by HRG-β1, we speculate that the observed HRG-β1-stimulated Akt activation was mainly mediated by ErbB3 receptors. On the other hand, HRG-β1 and HB-EGF demonstrated distinct patterns of ERK1/2 activation. Compared with JM-a/CYT-1 cells, HB-EGF selectively induced ERK1/2 phosphorylation in JM-a/CYT-2 cells at early time points (30 min to 4 h), followed by deactivation at a later time point (20 h). All three cell lines expressed high basal levels of phospho-STAT3, which were not further stimulated by either HRG-β1 or HB-EGF (Figure 8).

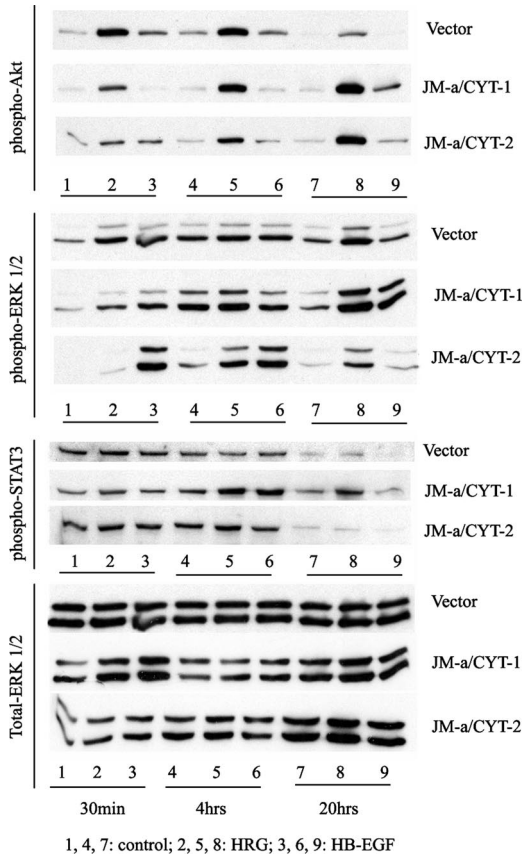

Figure 8. Effects of HRG-β1 and HB-EGF on phosphorylation of Akt, ERK 1/2, and STAT3. Quiescent cells were trypsinized and plated into 3D collagen gel mixture at 60,000 cells per 100 μl gel mixture with or without HRG-β1 or HB-EGF (50 ng/ml) treatment. Cells were lysed at the indicated time point, and cell lysates were resolved by 10% SDS-PAGE and subjected to immunoblotting with anti-phospho-Akt antibody, anti-phospho-ERK 1/2 antibody, or anti-phospho-STAT3 antibody. The membranes were then stripped and reprobed with anti-total ERK 1/2 antibody as a loading control.

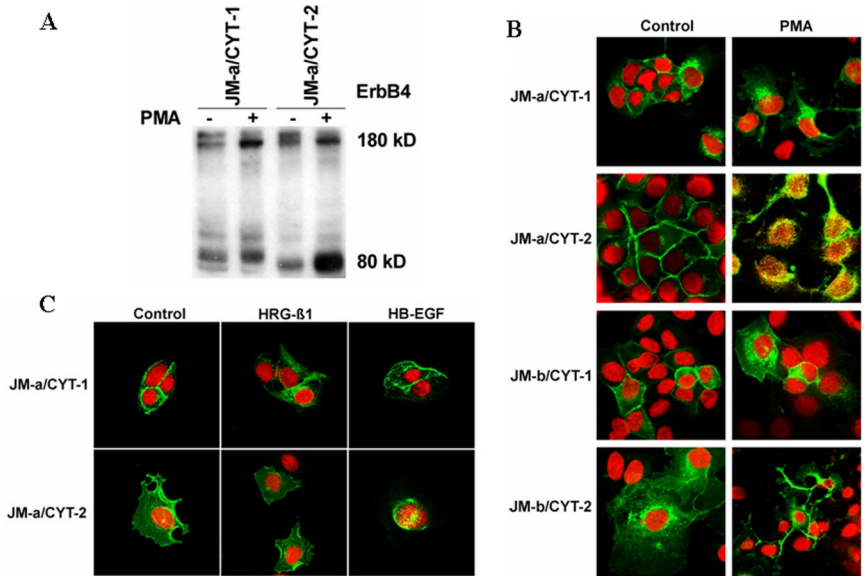

Figure 9. Cleavage and nuclear translocation of ErbB4 isoforms. (A) ErbB4 cleavage after PMA treatment. Cells were treated with 100 ng/ml PMA for 1 h. After SDS-PAGE and transfer to PVDF membrane, the samples were immunoblotted with anti-ErbB-4. (B and C) ErbB4 subcellular localization in response to PMA, HRG-β1, or HB-EGF treatment. ErbB4 isoform-transfected MDCK II cells were grown on coverslips, and cells were incubated with 10 ng/ml leptomycin B (LMB) for 12 h, an inhibitor of nuclear export, before treated with or without (as control) PMA (B) or HRG-β1 or HB-EGF (C) for 1 h. Subcellular localization of an intracellular ErbB4 epitope was determined by confocal microscopy. Green, ErbB4 staining; red, nuclei stained with TO-PRO-3.

ErbB4 JM-a/CYT-2 Isoform Translocated to Cell Nucleus in Response to HB-EGF Stimulation

Although both JM-a/CYT-1 and JM-a/CYT-2 cells could be cleaved upon ligand stimulation, HB-EGF induced tubulogenesis only in JM-a/CYT-2 cells. Furthermore, HB-EGF was unable to induce tubulogenesis in either of the JM-b cells. These results suggested that although ErbB4 cleavage was involved in this process, JM-a/CYT-2 receptors mediated specific responses required for tubulogenesis. Recent studies indicated that ErbB4 JM-a/CYT-2 and JM-a/CYT-1 isoforms exhibit different nuclear localization in human breast cancer cells (Maatta *et al.*, 2006), suggesting a possible mechanism to explain the different responses of the JM-a isoforms. We therefore examined nuclear localization of the cytoplasmic tail of JM-a/CYT-1 and JM-a/CYT-2 in the transfected MDCK cells in response to stimulation with phorbol ester, PMA, which can induce proteolytic cleavage of ErbB4 JM-a isoforms (Vecchi *et al.*, 1996). ErbB4 expressing cells incubated with or without 100 ng/ml PMA for 1 h at 37°C were tested for ErbB4 cleavage by Western blot and ErbB4 localization by immunofluorescence staining. As expected, PMA treatment increased expression of the 80-kDa fragment of both isoforms (Figure 9A). All four ErbB4 isoforms were primarily located at the plasma membrane and in the cytosol in the absence of PMA treatment. After PMA treatment, the JM-a/CYT-2 isoform selectively translocated to the nucleus, whereas in JM-a/CYT-1 cells, ErbB4 immunoreactivity was detected in the cytosol and perinuclear regions. As expected, PMA did not significantly alter localization of either JM-b/CYT-1 or JM-b/CYT-2 (Figure 9B). Of interest, HB-EGF also selectively induced nuclear translocation of the JM-a/CYT-2 isoform, whereas HRG-β1 failed to induce nuclear translocation of either JM-a isoform (Figure 9C).

DISCUSSION

ErbB4 is highly expressed in developing ductal epithelium, especially the terminal ducts and end buds in breast, where it has been suggested to play a role in regulating terminal differentiation of the mammary gland (Schroeder and Lee, 1998; Srinivasan *et al.*, 1998; Jones *et al.*, 1999). The metanephric kidney, which is also primarily comprised of branching ductal epithelial structures, requires soluble factors, including members of the EGF family, for normal development. Our previous studies showed that HB-EGF protein was expressed in the ureteric bud of embryonic kidneys. HB-EGF also induces branching tubulogenesis in cultured mouse UB cells (Takemura *et al.*, 2001). In addition to HB-EGF, we have determined that HRG-β1 is also expressed in the ureteric buds. Both HB-EGF and HRG-β1 can signal through activation of ErbB4. Thus the localization of ErbB4 and its ligands at ureteric bud suggests that ErbB4 may play a role in renal tubule development.

Consistent with previous reports (Kainulainen *et al.*, 2000), we found that the main ErbB4 isoforms in rat kidney were JM-a and CYT-2. Another noncleavable isoform, JM-c, which does not contain either JM-a or JM-b sequence, was also detected after E19, but in relatively lower amounts when compared with the JM-a isoform. On the other hand, the CYT-1 isoform was detected in early renal development stage from E15 to P6. These results suggest that during nephric development, different ErbB4 isoforms may be involved in nephrogenic processes and may act in coordination with each other.

The organization of polarized epithelia into architecturally distinct tubules is a characteristic feature of the mammalian kidney and is central to its physiological functions (Dressler, 2002). In this regard, we have utilized a well-described system of growth of MDCK II cells in collagen gels to recapitulate the events of branching morphogenesis. We demonstrated that in MDCK II cells, ErbB4 isoforms manifested 1) impaired cyst formation; 2) different defects in tubulogenesis upon HGF treatment, with JM-a/CYT-1 and JM-b/CYT-2 cells demonstrating elongated tubules without branching, JM-a/CYT-2 cells exhibiting scattered cells with extensive cell protrusions, and JM-b/CYT-1 cells producing coil-coiled tubule-like cysts; 3) responses to HRG-β1 treatment by rescuing cyst growth; and 4) ErbB4 JM-a/CYT-2 isoform, which lacks the PI3K-binding domain, induced branching tubule formation upon HB-EGF administration.

Tubulogenesis involves the coordination of a number of cellular functions, including cell proliferation, adhesion, migration, and apoptosis. Consistent with a role for ErbB4 in

inhibiting proliferation and/or inducing differentiation in other cell types (Srinivasan *et al.*, 2000; Ni *et al.*, 2001; Sartor et al., 2001), we determined that ErbB4 isoform expression significantly inhibited MDCK II cell proliferation in 3D collagen gel culture (Figure 6A), which may be the underlying reason for the poor cyst formation in the control group. HRG-β1 did stimulate proliferation in the ErbB4-overexpressing cells, as was indicated by the cyst formation and cell proliferation assays, but could not promote MDCK II tubulogenesis. Consistent with previous studies (Barros *et al.*, 1995), EGF was also unable to induce tubulogenesis in MDCK II cells with overexpression of vector alone or any of the ErbB4 isoforms. In contrast, in response to HB-EGF, only the JM-a/CYT-2 ErbB4 cells formed tubules, whereas vector-transfected cells and the other ErbB4 isoforms only formed cysts. Because HB-EGF can bind to both EGFR and ErbB4, the tubule formation seen in response to HB-EGF treatment in JM-a/CYT-2 cells suggested that a balance between activation of both EGFR and ErbB4 might be required for tubulogenesis. However, because this response was not seen with the other ErbB4 isoforms, it further suggested that the cleaved JM-a/CYT-2 intracellular domain (ICD-JM-a/CYT-2) may play a role, because HB-EGF selectively led to an increase in the cleaved phosphorylated cytoplasmic fragment of JM-a/CYT-2 (Figure 4C).

The different responses of JM-a/CYT-2 and JM-b/CYT-2 isoforms to HB-EGF suggested that the JM-a/CYT-2-mediated tubule formation was related to ErbB4 cleavage, which is the only difference between those two isoforms. On the other hand, even though both ErbB4 JM-a/CYT-1 and JM-a/CYT-2 isoforms are cleaved after activation, no branching tubule formation was detected in response to HB-EGF treatment in JM-a/CYT-1 cells. As previously noted, ICD-JM-a/CYT-1 contains a PI3K-binding domain and a WW-binding motif that are absent in ICD-JM-a/CYT-2. Compared with HRG-β1, we detected less phospho-Akt activation upon HB-EGF treatment in both JM-a/CYT-1 and JM-a/CYT-2, suggesting that differential PI3K binding and/or activation of PI3K/Akt pathway were not involved in the tubule formation in this situation. On the other hand, HB-EGF stimulated ERK phosphorylation to a much greater extent in JM-a/CYT-2 cells compared with either JM-a/CYT-1– or vector-transfected cells. Strong MAPK activation at early time points may facilitate MDCK epithelial-mesenchymal transition, an important step in tubulogenesis (O'Brien *et al.*, 2002).

Several studies have reported that WW-binding motifs in ErbB4 ICD may mediate subcellular localization of the cytoplasmic tail (Komuro et al., 2003; Omerovic et al., 2004). CYT-1 isoform cytoplasmic tails are more likely to be ubiquitinated and degraded in the proteosome, whereas CYT-2 isoform cytoplasmic tails are less likely to be degraded and can translocate to the nucleus (Maatta *et al.*, 2006). In agreement with these studies, we found that when the different ErbB4 isoforms were treated with PMA to induce cleavage of the JM-a isoforms, only JM-a/CYT-2 was translocated to the nucleus. Furthermore, the two ErbB4 ligands differentially affected nuclear translocation. HB-EGF, which induced tubulogenesis, selectively induced nuclear translocation of the JM-a/CYT-2 isoform of ErbB4, whereas there was no nuclear translocation in response to HRG-β1 treatment. At present, we do not understand this failure of HRG-β1 to induce nuclear localization but speculate it may be due to different intracellular signaling in response to simultaneous activation of ErbB3 (HRG-β1) versus ErbB1 (HB-EGF).

Initiation of multiple downstream signaling cascades in response to ligand-dependent formation of homo- or heterodimeric ErbB receptor complex formation has been well described. Recently, an alternative direct signaling mechanism has been proposed for ErbB4 (Ni *et al.*, 2001; Lee *et al.*, 2002). After TACE-dependent cleavage of the ErbB4 extracellular domain, regulated intracellular proteolysis produces a soluble ICD of ErbB4, which can be translocated to the nucleus and may possess transcriptional activity (Ni *et al.*, 2001; Lee *et al.*, 2002; Komuro *et al.*, 2003; Williams *et al.*, 2004). In other cell types, ErbB4 has been shown to facilitate nuclear translocation of other transcription factors, including STAT5a, YAP65 (Omerovic *et al.*, 2004; Muraoka-Cook *et al.*, 2006), and TAB2 and N-Cor (Sardi *et al.*, 2006). Therefore, we propose that the increased nuclear translocation of JM-a/CYT-2 cells may serve to mediate complex cellular responses, such as increased cell–matrix adhesion, cell motility, and cell proliferation, to modulate MDCK II tubulogenesis. Further studies will be required to determine which transcriptional factors are involved in the observed HB-EGF–induced tubulogenesis.

In conclusion, we report that ErbB4 was mainly expressed in ureteric buds and their derivatives. Low levels of ErbB4 in adult kidney were detected primarily in collecting ducts. In the rat kidney, JM-a was the major ErbB4 juxtamembrane isoform and CYT-2 was the major cytoplasmic tail isoform. In MDCK II cells transfected with ErbB4 isoforms, we demonstrated that the ErbB4 JM-a/CYT-2 isoform, which is a cleavable isoforms that lacks the PI3K- and WW-domain–binding sites, exhibits rapid attachment, increased motility, and HB-EGF–induced tubulogenesis, suggesting it may play a role in renal tubule development.

ACKNOWLEDGMENTS

This work was supported by funds from the Department of Veterans Affairs (R.H., R.Z.) and National Institutes of Health Grant DK51265 (R.H.) and DK69921 (R.Z.).

REFERENCES

Balkovetz, D. F. (1998). Hepatocyte growth factor and Madin-Darby canine kidney cells: in vitro models of epithelial cell movement and morphogenesis. Microsc. Res. Tech. *43,* 456–463.

Barros, E. J., Santos, O. F., Matsumoto, K., Nakamura, T., and Nigam, S. K. (1995). Differential tubulogenic and branching morphogenetic activities of growth factors: implications for epithelial tissue development. Proc. Natl. Acad. Sci. USA *92,* 4412–4416.

Beerli, R. R., and Hynes, N. E. (1996). Epidermal growth factor-related peptides activate distinct subsets of ErbB receptors and differ in their biological activities. J. Biol. Chem. *271,* 6071–6076.

Boccaccio, C., Ando, M., Tamagnone, L., Bardelli, A., Michieli, P., Battistini, C., and Comoglio, P. M. (1998). Induction of epithelial tubules by growth factor HGF depends on the STAT pathway. Nature *391,* 285–288.

Brader, S., and Eccles, S. A. (2004). Phosphoinositide 3-kinase signalling pathways in tumor progression, invasion and angiogenesis. Tumori *90,* 2–8.

Cantley, L. G., Barros, E. J., Gandhi, M., Rauchman, M., and Nigam, S. K. (1994). Regulation of mitogenesis, motogenesis, and tubulogenesis by hepatocyte growth factor in renal collecting duct cells. Am. J. Physiol. *267,* F271–F280.

Carpenter, G. (2003). ErbB-4, mechanism of action and biology. Exp. Cell Res. *284,* 66–77.

Chen, D. *et al.* (2004). Differential expression of collagen- and laminin-binding integrins mediates ureteric bud and inner medullary collecting duct cell tubulogenesis. Am. J. Physiol. Renal Physiol. *287,* F602–F611.

Cheng, Q. C., Tikhomirov, O., Zhou, W., and Carpenter, G. (2003). Ectodomain cleavage of ErbB- 4, characterization of the cleavage site and m80 fragment. J. Biol. Chem. *278,* 38421–38427.

Dressler, G. (2002). Tubulogenesis in the developing mammalian kidney. Trends Cell Biol. *12,* 390–395.

Elenius, K., Choi, C. J., Paul, S., Santiestevan, E., Nishi, E., and Klagsbrun, M. (1999). Characterization of a naturally occurring ErbB4 isoform that does not bind or activate phosphatidyl inositol 3-kinase. Oncogene *18,* 2607–2615.

Elenius, K., Corfas, G., Paul, S., Choi, C. J., Rio, C., Plowman, G. D., and Klagsbrun, M. (1997a). A novel juxtamembrane domain isoform of HER4/ErbB4. Isoform-specific tissue distribution and differential processing in response to phorbol ester. J. Biol. Chem. *272,* 26761–26768.

Elenius, K., Paul, S., Allison, G., Sun, J., and Klagsbrun, M. (1997b). Activation of HER4 by heparin-binding EGF-like growth factor stimulates chemotaxis but not proliferation. EMBO J. *16,* 1268–1278.

Falls, D. L. (2003). Neuregulins: functions, forms, and signaling strategies. Exp. Cell Res. *284,* 14–30.

Gassmann, M., Casagranda, F., Orioli, D., Simon, H., Lai, C., Klein, R., and Lemke, G. (1995). Aberrant neural and cardiac development in mice lacking the ErbB4 neuregulin receptor. Nature *378,* 390–394.

Gilbertson, R., Hernan, R., Pietsch, T., Pinto, L., Scotting, P., Allibone, R., Ellison, D., Perry, R., Pearson, A., and Lunec, J. (2001). Novel ERBB4 juxtamembrane splice variants are frequently expressed in childhood medulloblastoma. Genes Chromosomes Cancer *31,* 288–294.

Gilmour, L. M., Macleod, K. G., McCaig, A., Gullick, W. J., Smyth, J. F., and Langdon, S. P. (2001). Expression of erbB-4/HER-4 growth factor receptor isoforms in ovarian cancer. Cancer Res. *61,* 2169–2176.

Grant, S., Qiao, L., and Dent, P. (2002). Roles of ERBB family receptor tyrosine kinases, and downstream signaling pathways, in the control of cell growth and survival. Front. Biosci. *7,* d376–389.

Hotchkiss, K. A., Basile, C. M., Spring, S. C., Bonuccelli, G., Lisanti, M. P., and Terman, B. I. (2005). TEM8 expression stimulates endothelial cell adhesion and migration by regulating cell-matrix interactions on collagen. Exp. Cell Res. *305,* 133–144.

Jones, F. E., Welte, T., Fu, X. Y., and Stern, D. F. (1999). ErbB4 signaling in the mammary gland is required for lobuloalveolar development and Stat5 activation during lactation. J. Cell Biol. *147,* 77–88.

Kainulainen, V., Sundvall, M., Maatta, J. A., Santiestevan, E., Klagsbrun, M., and Elenius, K. (2000). A natural ErbB4 isoform that does not activate phosphoinositide 3-kinase mediates proliferation but not survival or chemotaxis. J. Biol. Chem. *275,* 8641–8649.

Komuro, A., Nagai, M., Navin, N. E., and Sudol, M. (2003). WW domain-containing protein YAP associates with ErbB-4 and acts as a co-transcriptional activator for the carboxyl-terminal fragment of ErbB-4 that translocates to the nucleus. J. Biol. Chem. *278,* 33334–33341.

Lee, H. J., Jung, K. M., Huang, Y. Z., Bennett, L. B., Lee, J. S., Mei, L., and Kim, T. W. (2002). Presenilin-dependent gamma-secretase-like intramembrane cleavage of ErbB4. J. Biol. Chem. *277,* 6318–6323.

Maatta, J. A., Sundvall, M., Junttila, T. T., Peri, L., Laine, V. J., Isola, J., Egeblad, M., and Elenius, K. (2006). Proteolytic cleavage and phosphorylation of a tumor-associated ErbB4 isoform promote ligand-independent survival and cancer cell growth. Mol. Biol. Cell *17,* 67–79.

Mai, W. *et al.* (2005). Inhibition of Pkhd1 impairs tubulomorphogenesis of cultured IMCD cells. Mol. Biol. Cell *16,* 4398–4409.

Medico, E., Mongiovi, A. M., Huff, J., Jelinek, M. A., Follenzi, A., Gaudino, G., Parsons, J. T., and Comoglio, P. M. (1996). The tyrosine kinase receptors Ron and Sea control "scattering" and morphogenesis of liver progenitor cells in vitro. Mol. Biol. Cell *7,* 495–504.

Montesano, R., Schaller, G., and Orci, L. (1991). Induction of epithelial tubular morphogenesis in vitro by fibroblast-derived soluble factors. Cell *66,* 697–711.

Muraoka-Cook, R. S., Sandahl, M., Husted, C., Hunter, D., Miraglia, L., Feng, S. M., Elenius, K., and Earp, H. S., 3rd. (2006). The intracellular domain of ErbB4 induces differentiation of mammary epithelial cells. Mol. Biol. Cell *17,* 4118–4129.

Ni, C. Y., Murphy, M. P., Golde, T. E., and Carpenter, G. (2001). gamma-Secretase cleavage and nuclear localization of ErbB-4 receptor tyrosine kinase. Science *294,* 2179–2181.

O'Brien, L. E., Tang, K., Kats, E. S., Schutz-Geschwender, A., Lipschutz, J. H., and Mostov, K. E. (2004). ERK and MMPs sequentially regulate distinct stages of epithelial tubule development. Dev. Cell *7,* 21–32.

O'Brien, L. E., Zegers, M. M., and Mostov, K. E. (2002). Opinion: Building epithelial architecture: insights from three-dimensional culture models. Nat. Rev. Mol. Cell Biol. *3,* 531–537.

Olayioye, M. A., Neve, R. M., Lane, H. A., and Hynes, N. E. (2000). The ErbB signaling network: receptor heterodimerization in development and cancer. EMBO J. *19,* 3159–3167.

Omerovic, J., Puggioni, E. M., Napoletano, S., Visco, V., Fraioli, R., Frati, L., Gulino, A., and Alimandi, M. (2004). Ligand-regulated association of ErbB-4 to the transcriptional co-activator YAP65 controls transcription at the nuclear level. Exp. Cell Res. *294,* 469–479.

Ponzetto, C., Zhen, Z., Audero, E., Maina, F., Bardelli, A., Basile, M. L., Giordano, S., Narsimhan, R., and Comoglio, P. (1996). Specific uncoupling of GRB2 from the Met receptor. Differential effects on transformation and motility. J. Biol. Chem. *271,* 14119–14123.

Pozzi, A. *et al.* (2006). H-Ras, R-Ras, and TC21 differentially regulate ureteric bud cell branching morphogenesis. Mol. Biol. Cell *17,* 2046–2056.

Ridley, A. J., Comoglio, P. M., and Hall, A. (1995). Regulation of scatter factor/hepatocyte growth factor responses by Ras, Rac, and Rho in MDCK cells. Mol. Cell. Biol. *15,* 1110–1122.

Riese, D. J., 2nd, Bermingham, Y., van Raaij, T. M., Buckley, S., Plowman, G. D., and Stern, D. F. (1996). Betacellulin activates the epidermal growth factor receptor and erbB-4, and induces cellular response patterns distinct from those stimulated by epidermal growth factor or neuregulin-beta. Oncogene *12,* 345–353.

Riese, D. J., 2nd, and Stern, D. F. (1998). Specificity within the EGF family/ErbB receptor family signaling network. Bioessays *20,* 41–48.

Rio, C., Buxbaum, J. D., Peschon, J. J., and Corfas, G. (2000). Tumor necrosis factor-alpha-converting enzyme is required for cleavage of erbB4/HER4. J. Biol. Chem. *275,* 10379–10387.

Royal, I., and Park, M. (1995). Hepatocyte growth factor-induced scatter of Madin-Darby canine kidney cells requires phosphatidylinositol 3-kinase. J. Biol. Chem. *270,* 27780–27787.

Sachs, M., Weidner, K. M., Brinkmann, V., Walther, I., Obermeier, A., Ullrich, A., and Birchmeier, W. (1996). Motogenic and morphogenic activity of epithelial receptor tyrosine kinases. J. Cell Biol. *133,* 1095–1107.

Sakai, M., Zhang, M., Homma, T., Garrick, B., Abraham, J. A., McKanna, J. A., and Harris, R. C. (1997). Production of heparin binding epidermal growth factor-like growth factor in the early phase of regeneration after acute renal injury. Isolation and localization of bioactive molecules. J. Clin. Invest. *99,* 2128–2138.

Santos, O. F., and Nigam, S. K. (1993). HGF-induced tubulogenesis and branching of epithelial cells is modulated by extracellular matrix and TGF-beta. Dev. Biol. *160,* 293–302.

Sardi, S. P., Murtie, J., Koirala, S., Patten, B. A., and Corfas, G. (2006). Presenilin-dependent ErbB4 nuclear signaling regulates the timing of astrogenesis in the developing brain. Cell *127,* 185–197.

Sartor, C. I. *et al.* (2001). Her4 mediates ligand-dependent antiproliferative and differentiation responses in human breast cancer cells. Mol. Cell. Biol. *21,* 4265–4275.

Schroeder, J. A., and Lee, D. C. (1998). Dynamic expression and activation of ERBB receptors in the developing mouse mammary gland. Cell Growth Differ. *9,* 451–464.

Srinivasan, R., Gillett, C. E., Barnes, D. M., and Gullick, W. J. (2000). Nuclear expression of the c-erbB-4/HER-4 growth factor receptor in invasive breast cancers. Cancer Res. *60,* 1483–1487.

Srinivasan, R., Poulsom, R., Hurst, H. C., and Gullick, W. J. (1998). Expression of the c-erbB-4/HER4 protein and mRNA in normal human fetal and adult tissues and in a survey of nine solid tumour types. J. Pathol. *185,* 236–245.

Stuart, R. O., Barros, E. J., Ribeiro, E., and Nigam, S. K. (1995). Epithelial tubulogenesis through branching morphogenesis: relevance to collecting system development. J. Am. Soc. Nephrol. *6,* 1151–1159.

Takemura, T., Hino, S., Kuwajima, H., Yanagida, H., Okada, M., Nagata, M., Sasaki, S., Barasch, J., Harris, R. C., and Yoshioka, K. (2001). Induction of collecting duct morphogenesis in vitro by heparin-binding epidermal growth factor-like growth factor. J. Am. Soc. Nephrol. *12,* 964–972.

Takemura, T., Hino, S., Okada, M., Murata, Y., Yanagida, H., Ikeda, M., Yoshioka, K., and Harris, R. C. (2002). Role of membrane-bound heparin-binding epidermal growth factor-like growth factor (HB-EGF) in renal epithelial cell branching. Kidney Int. *61,* 1968–1979.

Vecchi, M., Baulida, J., and Carpenter, G. (1996). Selective cleavage of the heregulin receptor ErbB-4 by protein kinase C activation. J. Biol. Chem. *271,* 18989–18995.

Vecchi, M., and Carpenter, G. (1997). Constitutive proteolysis of the ErbB-4 receptor tyrosine kinase by a unique, sequential mechanism. J. Cell Biol. *139,* 995–1003.

Williams, C. C., Allison, J. G., Vidal, G. A., Burow, M. E., Beckman, B. S., Marrero, L., and Jones, F. E. (2004). The ERBB4/HER4 receptor tyrosine kinase regulates gene expression by functioning as a STAT5A nuclear chaperone. J. Cell Biol. *167*, 469–478.

Yarden, Y., and Sliwkowski, M. X. (2001). Untangling the ErbB signalling network. Nat. Rev. Mol. Cell Biol. *2,* 127–137.

Zhang, M. Z., Sanchez Lopez, P., McKanna, J. A., and Harris, R. C. (2004). Regulation of cyclooxygenase expression by vasopressin in rat renal medulla. Endocrinology *145,* 1402–1409.

Zhou, W., and Carpenter, G. (2000). Heregulin-dependent trafficking and cleavage of ErbB-4. J. Biol. Chem. *275,* 34737–34743.